Realizable receivers for discriminating coherent and multicopy quantum states near the quantum limit

Ranjith Nair,[1] Saikat Guha,[2] and Si-Hui Tan[3]

[1]*Department of Electrical and Computer Engineering, National University of Singapore, 4 Engineering Drive 3, Singapore 117583*

[2]*Quantum Information Processing group, Raytheon BBN Technologies, Cambridge, Massachusetts 02138*

[3]*Singapore University of Technology and Design, 20 Dover Dr, Singapore 138682*

(Received 16 July 2013; published 12 March 2014)

We derive the quantum limit on the error probability exponent for discriminating any M multimode coherent states of light and show that it is four times that of an ideal heterodyne receiver for the same signal set. We then propose a receiver that achieves the quantum limit using auxiliary coherent-state fields, beam splitters, and single-photon detectors. The performance of the receiver is compared to standard measurements for various imaging and communication tasks. A related receiver for discriminating arbitrary multicopy pure quantum states is shown to achieve the M-ary quantum Chernoff exponent and does so using only local operations and classical communication.

DOI: 10.1103/PhysRevA.89.032318 PACS number(s): 03.67.Hk, 42.50.Dv, 42.50.Ex

I. INTRODUCTION

Optimally discriminating unknown nonorthogonal quantum states using appropriate quantum measurements [1–4] is a basic primitive underlying many quantum information processing tasks such as communication [1], sensing and metrology [4–8], and cryptography [9–11]. The central problem of quantum detection theory [1] is to determine the quantum measurement, specified abstractly by a positive operator-valued measure (POVM) [4], that minimizes the average error probability in discriminating a given ensemble of states. The problem has been solved in terms of necessary and sufficient conditions that the optimal POVM must satisfy [12,13], but for discriminating more than two states, the explicit solution of these conditions is known only in very specific cases (see, e.g., Refs. [14–18]). The scope of quantum detection theory has since widened to include other scenarios such as unambiguous state discrimination, maximum confidence discrimination, and to discrimination using a quantum computer with limited entanglement [19].

The main motivation for this work is the design of concrete *receivers*, i.e., physical realizations of POVM's, for discriminating coherent states of light [20–38]. Coherent states [39] (and their mixtures) are the most ubiquitous quantum states of light and their discrimination is central to optical communication [40] and sensing [4,41]. The optimal error probability of discriminating an ensemble of coherent states decreases exponentially with the average energy (or equivalently, with the average photon number, in the narrowband case considered here) in the large-energy regime [1]. This is also true for the error probability of the standard direct, homodyne, and heterodyne detection receivers [40]. However, the exponent of the optimal receiver allowed by quantum mechanics is in general greater than that of the conventional measurements [1,20,21,31,33], leaving a gap between the optimal error probability (popularly called the *Helstrom limit*) and the minimum achievable by conventional measurements, viz., homodyne, heterodyne, and direct detection (loosely called *standard quantum limits*).

For discriminating two coherent states, the Kennedy receiver [20] is *exponentially optimal*, i.e., it achieves the maximum error probability exponent in the high-photon-number regime. Dolinar proposed a more complicated design that exactly achieves the Helstrom limit [21] and was demonstrated in a proof-of-principle experiment [22]. Sasaki and Hirota conceived a receiver that could achieve the Helstrom limit without using the fast electro-optic feedback required by the Dolinar receiver [23], but this design required unknown nonlinear-optical transformations, making it impractical. Receivers with performance in between the Kennedy and Dolinar receivers were recently proposed [26,27] and demonstrated [28–30] in the low-photon-number regime. Going beyond two states, Dolinar proposed an exponentially optimal receiver for M-ary pulse position modulation (PPM) [31] that was recently demonstrated experimentally [32]. Bondurant proposed an exponentially optimal receiver for the 4-ary phase shift keying (4-PSK) constellation [33]. Recently, Becerra *et al*. proposed and implemented a feedforward receiver structure for M-ary PSK that beats the heterodyne limit for 4-PSK [34,35]. Other receiver designs continue to be proposed and demonstrated for particular coherent-state ensembles [36,37].

A parallel motivation for this work lies in the theory of multicopy state discrimination using local operations and classical communication (LOCC) [42–47] in the limit of a large number of copies [48–52]. For discriminating between n identical copies of one of two density operators, the error probability of the optimal quantum measurement falls off exponentially with n with a characteristic exponent depending on the pair of states known as the quantum Chernoff exponent [48,49] in analogy with its classical version [53]. Although the measurement achieving this optimal scaling is expected to be a joint one over all n copies, for discriminating two pure states, the scaling and even the exact optimal error probability is obtainable by copy-by-copy measurements with successive measurements depending on previous results [43]. The case of two mixed states is less well understood, although there are examples of mixed qubit states for which a finite gap exists between the Chernoff exponent and the best exponent achievable using LOCC [44–47]. The theory of multicopy state discrimination was recently extended to $M > 2$ states in Refs. [50–52], where it was shown that the error probability scales exponentially with the number of copies with an

exponent not larger than the smallest of the pairwise Chernoff exponents between the states of the ensemble. For pure-state ensembles, a particular measurement was shown to achieve this exponent so as to make it the exact M-ary Chernoff exponent [50]. This achievability result was extended to some classes of mixed-state ensembles in Refs. [51,52].

Our contribution in this work is threefold. First, we use the *quantum Chernoff* exponent in M-ary multicopy state discrimination [50] to obtain the maximum *error probability* exponent with respect to the average signal energy allowed of a coherent-state receiver by quantum mechanics. We show that the exponent of the multimode heterodyne receiver is smaller in general than this optimal value by a factor of four. The Kennedy [20], Bondurant [33], and Becerra [34,35] receivers rely on a strategy of attempting to null—i.e., displace to the vacuum—the input state by successively subtracting the fields corresponding to the possible hypotheses. As our second contribution, we propose a receiver called the *sequential waveform nulling* (SWN) receiver for discriminating any ensemble of M, possibly multimode, coherent states. While the Helstrom measurement on a coherent-state ensemble appears in general to require a quantum computer [38], we show that the quantum limit on the error probability exponent obtained here is approached by the SWN receiver using only auxiliary coherent-state generation, beam splitters, and single-photon detection. The SWN receiver subsumes the Kennedy [20] and the Type-I Bondurant [33] receiver and is similar to the Becerra receivers [34,35] but requires no classical data processing.[1] To illustrate the capabilities of the SWN receiver, we consider an image discrimination task for which the error probability of the SWN receiver surpasses the heterodyne limit for energy N beyond a low value. Similar quantitative comparisons to standard receivers are made for the 4-PSK and 6-PPM signal sets. As our final contribution, we generalize the idea of sequential nulling to pure-state ensembles in an arbitrary Hilbert space, propose a multicopy discrimination strategy called the *sequential testing* (ST) receiver, and show that it attains the M-ary Chernoff exponent for multicopy discrimination derived in Ref. [50]. Unlike the joint measurement constructed in Ref. [50] for achieving the M-ary Chernoff exponent, the ST receiver makes only copy-by-copy binary projective measurements and is thus potentially realizable using current technology.

[1]In Ref. [33], Bondurant proposed two receivers ("Type I" and "Type II") for the 4-PSK signal set. The Type I receiver nulls hypotheses in a predetermined sequence, while the Type II receiver nulls hypotheses in an order depending on the times that counts were observed, thereby achieving a slightly improved performance. Similar to the latter receiver, the Becerra *et al*. receiver [34,35] nulls, after each detection stage, the most probable hypothesis conditioned on the previous detection data. In contrast, our SWN receiver nulls hypotheses in an arbitrary but predetermined sequence, and is therefore more akin to Bondurant's Type I receiver. However, our claim of asymptotic optimality is expected to carry over, *a fortiori*, to the more optimized strategies of the Becerra *et al*. receivers and Bondurant's Type II receiver. See also Ref. [47] for a discussion of various strategies to optimize local measurements in the context of binary state discrimination.

This paper is organized as follows: In Sec. II, we fix some notations and formally define the various error probability exponents studied in this paper. In Sec. III, we derive the Helstrom and heterodyne error probability exponents for general coherent-state ensembles, establishing that the former is four times the latter. In Sec. IV, we introduce our sequential waveform nulling receiver, describe its operation, obtain its error probability for general coherent-state ensembles, and show that its error probability exponent is nearly quantum optimal. We also study its performance on a multispatial-mode (image) ensemble, a single-mode (4-PSK) ensemble, and a multitemporal-mode (6-PPM) ensemble. In Sec. V, we introduce the sequential testing receiver for discriminating multicopy pure-state ensembles and show that it achieves the M-ary quantum Chernoff exponent. Finally, in Sec. VI, we put the results obtained here in perspective and discuss some applications and directions for future work.

II. NOTATION AND DEFINITIONS

Consider M narrow-band complex-valued coherent-state waveforms $\{\mathcal{E}_m(\boldsymbol{\rho},t)\}_{m=1}^M$, where $\boldsymbol{\rho}\in\mathcal{A}$ is the transverse spatial coordinate in the entrance pupil $\mathcal{A}$ of the receiver aperture plane and $t\in\mathcal{T}=[0,T]$ denotes time within the signaling interval $\mathcal{T}$.[2] The mth waveform corresponds to the mth hypotheses to be discriminated. The $\{\mathcal{E}_m(\boldsymbol{\rho},t)\}_{m=1}^M$ are expressed in units of $\sqrt{\text{photons}\,\text{m}^{-2}\,\text{s}^{-1}}$, can be completely arbitrary, and correspond to coherent states $\{|\boldsymbol{\alpha}_m\rangle=|\alpha_m^{(1)}\rangle\otimes\cdots\otimes|\alpha_m^{(S)}\rangle\}_{m=1}^M$ on the Hilbert space of $S\leqslant M$ orthonormal spatiotemporal modes $\{\phi_s(\boldsymbol{\rho},t)\}_{s=1}^S$ that span the waveform space. Classically, the mth waveform is represented as the point $\boldsymbol{\alpha}_m\in\mathbb{C}^S$ in an S-mode phase space [1,54]. Let

$$E_m=\int_{\mathcal{A}}\int_{\mathcal{T}}|\mathcal{E}_m(\boldsymbol{\rho},t)|^2d\boldsymbol{\rho}dt=\|\boldsymbol{\alpha}_m\|^2 \tag{1}$$

denote the average energy of the mth waveform in photon units, and let

$$\begin{aligned}\underline{\Delta}&:=\min_{m,m':m\neq m'}\int_{\mathcal{A}}\int_{\mathcal{T}}|\mathcal{E}_m(\boldsymbol{\rho},t)-\mathcal{E}_{m'}(\boldsymbol{\rho},t)|^2\,d\boldsymbol{\rho}dt\\&=\min_{m,m':m\neq m'}\|\boldsymbol{\alpha}_m-\boldsymbol{\alpha}_{m'}\|^2\,.\end{aligned} \tag{2}$$

Thus, $\underline{\Delta}$ is the minimum squared distance among each pair of signal points in phase space. For an a priori probability distribution $\{\pi_m\}_{m=1}^M$, the average energy N in the ensemble is given by

$$N=\sum_{m=1}^M\pi_mE_m. \tag{3}$$

The *error probability exponent* (EPE) $\xi^{\#}$ of a coherent-state receiver #, where # may denote, e.g., the optimal Helstrom (Hel) receiver, the heterodyne (Het) receiver, or the SWN receiver, is defined as

$$\xi^{\#}[\{\boldsymbol{\alpha}_m\}]:=-\lim_{N\to\infty}\frac{1}{N}\ln P_E^{\#}\big[\{\boldsymbol{\alpha}_m\}^{(N)}\big], \tag{4}$$

[2]For simplicity, we assume the waveforms all have the same polarization.

where $P_E^{\#}[\{\boldsymbol{\alpha}_m\}^{(N)}]$ is the average error probability of the receiver # used to discriminate the coherent-state ensemble $\{|\boldsymbol{\alpha}_m\rangle\}^{(N)}$ consisting of waveforms proportional to the given set $\{\boldsymbol{\alpha}_m\}_{m=1}^M$ but uniformly scaled to have average energy N. This definition is simply a translation to coherent-state discrimination of the standard notion of error probability exponent in classical digital communication. The EPE is a key figure of merit for a receiver—a larger exponent indicates better performance.

For an ensemble $\mathcal{F} = \{\rho_m\}_{m=1}^M$ of states from an arbitrary Hilbert space, consider the n-copy ensemble $\mathcal{F}^{\otimes n} = \{\rho_m^{\otimes n}\}_{m=1}^M$. The *quantum Chernoff exponent* (QCE) $\xi_{\mathrm{QC}}[\mathcal{F}]$ of $\mathcal{F}$ is defined as [50,51]

$$\xi_{\mathrm{QC}}[\mathcal{F}] := -\lim_{n\to\infty} \frac{1}{n} \ln P_E^{\mathrm{Hel}}[\mathcal{F}^{\otimes n}], \tag{5}$$

where $P_E^{\mathrm{Hel}}[\mathcal{F}^{\otimes n}]$ is the average error probability of the *Helstrom* receiver discriminating the ensemble $\mathcal{F}^{\otimes n}$. For pure-state ensembles $\mathcal{F} = \{|\psi_m\rangle\}_{m=1}^M$, we have [50]

$$\xi_{\mathrm{QC}}[\mathcal{F}] = \min_{m,m':m\neq m'} -\ln |\langle\psi_m|\psi_{m'}\rangle|^2. \tag{6}$$

III. OPTIMAL AND HETERODYNE EXPONENTS IN COHERENT-STATE DISCRIMINATION

The EPE of the Helstrom measurement on a coherent-state ensemble $\{\boldsymbol{\alpha}_m\}$ is, by definition,

$$\xi^{\mathrm{Hel}}[\{\boldsymbol{\alpha}_m\}] := -\lim_{N\to\infty} \frac{1}{N} \ln P_E^{\mathrm{Hel}}\big[\{\boldsymbol{\alpha}_m\}^{(N)}\big] \tag{7}$$

$$= -\lim_{n\to\infty} \frac{1}{n} \ln P_E^{\mathrm{Hel}}\big[\otimes^n \{\boldsymbol{\alpha}_m\}^{(1)}\big] \tag{8}$$

$$= \xi_{\mathrm{QC}}\big[\{\boldsymbol{\alpha}_m\}^{(1)}\big] = \underline{\Delta}/N \equiv \kappa. \tag{9}$$

In Eq. (8), n has been restricted to integer values and Eq. (8) follows because a coherent-state ensemble can be split into n identical copies using a unitary beam splitter transformation and because this action cannot change the error probability of the Helstrom receiver. We are now in the multicopy discrimination framework and the left-most term in Eq. (9) follows from Eq. (6), and we have used the coherent-state overlap $|\langle\boldsymbol{\alpha}_m|\boldsymbol{\alpha}_{m'}\rangle|^2 = e^{-\|\boldsymbol{\alpha}_m-\boldsymbol{\alpha}_{m'}\|^2}$ to get the second equality of Eq. (9). We have also defined the N-independent constant κ that is a function of the prior probability distribution and the ensemble $\{\boldsymbol{\alpha}_m\}$ up to a scale factor, i.e., an ensemble $\{\boldsymbol{\alpha}'_m = \lambda\boldsymbol{\alpha}_m\}$ with the same prior probability distribution has the same κ as $\{\boldsymbol{\alpha}_m\}$.

Heterodyning each of the S modes on which the ensemble is supported yields, conditional on the state $|\boldsymbol{\alpha}_m\rangle$, an observation in $\mathbb{C}^S$ with mean value $\boldsymbol{\alpha}_m$ and added zero-mean white Gaussian noise of variance $1/2$ in each of $2S$ quadratures of the S modes. For this essentially classical situation, the M-ary Chernoff exponent equals the smallest binary Chernoff exponent between all pairs of the hypotheses [51,55]. The latter quantity is well known in the Gaussian-noise case [56] and results in

$$\xi^{\mathrm{Het}}[\{\boldsymbol{\alpha}_m\}] = \frac{\Delta}{4N} = \frac{\kappa}{4}, \tag{10}$$

so that the heterodyne EPE is a factor of four worse than the Helstrom EPE regardless of the ensemble $\{|\boldsymbol{\alpha}_m\rangle\}$.

IV. SEQUENTIAL WAVEFORM NULLING RECEIVER

A. Operation

The sequential waveform nulling (SWN) receiver (Fig. 1) operates as follows: To begin with, the signal field over $\mathcal{A}\times\mathcal{T}$ is split into L equal-amplitude portions or *slices* [L may be arbitrarily large but at least equal to $(M-1)$] that are placed in lossless storage, e.g., the fiber loop in Fig. 1, and are accessed and sequentially processed as follows:

(1) Initialize the *slice number* l to $l = 1$.
(2) Initialize the *nulled hypothesis* μ to $\mu = 1$.
(3) While $l \leqslant L$
  (a) Displace the lth slice of the input field by the field $-\frac{\mathcal{E}_\mu(\boldsymbol{\rho},t)}{\sqrt{L}}$ and direct detect the output field in $\mathcal{A}\times\mathcal{T}$ on a single-photon detector.
  (b) If the detector clicks, set $\mu := \mu + 1$.
  (c) $l := l + 1$.
(4) Set the receiver's decision $\hat{m} := \mu$.

As shown below, the L-fold amplitude-slicing enables the SWN receiver to achieve the optimal exponent for hypotheses in *arbitrary* spatiotemporal modes in the limit of large L. In practice, due to the finite bandwidth for switching of the LO pattern and the finite dead time of the detector after the detection of a photon, the next slice cannot be processed immediately after a detector click. If it is held in storage until the LO waveform and detector are reset, the portion of the input state in this interval is not lost, provided storage loss can be neglected. In effect, such a splitting strategy was used, albeit with a different architecture than Fig. 1, in the experiments of Ref. [34,35] (our "slices" correspond to the "stages" of Refs. [34,35]).

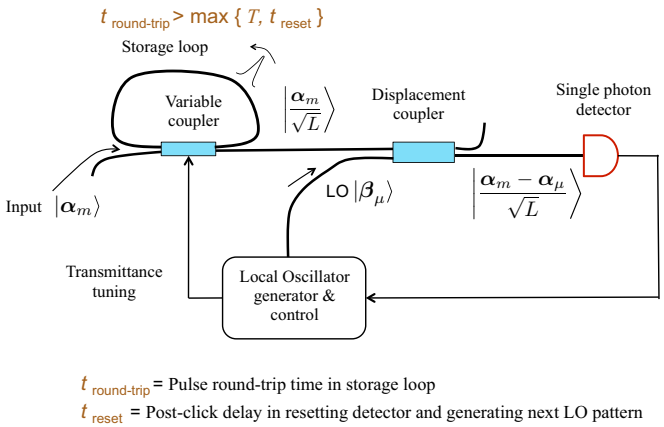

FIG. 1. (Color online) A possible implementation of the SWN receiver. The variable coupler taps a $1/L$th fraction of the input energy after each round trip around the fiber loop. Each slice is displaced by the negative of one of the scaled hypotheses at the displacement coupler and the local oscillator (LO) field pattern is switched to match the next hypothesis for the next slice whenever the single-photon detector registers a count. Additional elements necessary to keep the LO amplitude and phase coherent with those of the input are not shown.

B. General error probability analysis

We now derive an expression for the error probability of the SWN receiver for an arbitrary coherent-state ensemble, obtain an upper bound on it [Eq. (18) below], and use it to derive the lower bound [Eq. (19) below] on the SWN error probability exponent.

The error probability analysis of the SWN receiver, based as it is on direct detection of coherent states, can be carried out using the semiclassical theory of photodetection [40,54] and proceeds as follows: From the method of operation of the receiver described in the previous section, it is apparent that when the mth hypothesis is true, we cannot get more than $m-1$ total clicks over the L slices. Further, if $m-1$ clicks are observed, we declare correctly that hypothesis m is true. We thus have for the conditional probability of error given that hypothesis m is true

$$P^{\mathrm{SWN}}[E|m] = \sum_{K=0}^{m-2} \Pr[K \text{ clicks are observed} \mid m], \tag{11}$$

where the $m=1$ case may be included by agreeing that sums in which the starting value of the summation index exceeds the ending value are zero. For $K>0$, the summand may be written as follows: the $K=0$ case is dealt with later. Define a length-K vector $\mathbf{l}=(l_1,\ldots,l_K)$ whose kth component l_k is the slice number in the detection of which the kth click occurred. The possible instances of $\mathbf{l}$ are the increasing sequences of K integers chosen from $\{1,\ldots,L\}$, and are thus $\binom{L}{K}$ in number. When the nulled hypothesis is $\mu<m$, the average number of photons incident on the detector in one slice is $\Delta_{\mu,m}/L$, where

$$\begin{aligned}\Delta_{m,m'} &:= \int_{\mathcal{A}}\int_{\mathcal{T}} |\mathcal{E}_m(\boldsymbol{\rho},t)-\mathcal{E}_{m'}(\boldsymbol{\rho},t)|^2\, d\boldsymbol{\rho}dt \\ &= \|\boldsymbol{\alpha}_m-\boldsymbol{\alpha}_{m'}\|^2 .\end{aligned} \tag{12}$$

We may then write, using the Poisson statistics of detection in each slice together with the conditional statistical independence of photon counts in successive slices,

$$\begin{aligned}&\Pr[K \text{ clicks are observed} \mid m] \\ &= \sum_{\text{allowed}\mathbf{l}} \exp\left\{-\Delta_{1,m}\frac{(l_1-1)}{L}\right\}\left(1-\exp\left\{-\frac{\Delta_{1,m}}{L}\right\}\right) \\ &\quad\times \exp\left\{-\Delta_{2,m}\frac{(l_2-l_1-1)}{L}\right\}\left(1-\exp\left\{-\frac{\Delta_{2,m}}{L}\right\}\right)\times\cdots \\ &\quad\times \exp\left\{-\Delta_{K,m}\frac{(l_K-l_{K-1}-1)}{L}\right\}\left(1-\exp\left\{-\frac{\Delta_{K,m}}{L}\right\}\right) \\ &\quad\times \exp\left\{-\Delta_{K+1,m}\frac{(L-l_K)}{L}\right\},\end{aligned} \tag{13}$$

where factors of the form $\exp\{\cdot\}$ are probabilities that no clicks are obtained in the intervals between the click locations indicated by $\mathbf{l}$ while factors of the form $(1-\exp\{\cdot\})$ are probabilities of obtaining a click in the click locations. With the conventions $l_0:=0$ and $l_{K+1}:=L+1$, we may rewrite and bound the above expression as follows:

$$\begin{aligned}&\Pr[K \text{ clicks are observed} \mid m] \\ &\leqslant \sum_{\text{allowed}\mathbf{l}}\prod_{k=0}^{K}\exp\left\{-\Delta_{k+1,m}\frac{l_{k+1}-l_k-1}{L}\right\} &(14)\\ &\leqslant \sum_{\text{allowed}\mathbf{l}}\prod_{k=0}^{K}\exp\left\{-\underline{\Delta}\frac{l_{k+1}-l_k-1}{L}\right\} &(15)\\ &= \binom{L}{K}\exp\left\{-\underline{\Delta}\frac{(L-K)}{L}\right\}. &(16)\end{aligned}$$

To get Eq. (15), we have used the definition (2) of $\underline{\Delta}$. For $K=0$ and for $m>1$, we have $\Pr[K \text{ clicks are observed} \mid m] = \exp(-\Delta_{1,m}) \leqslant \exp(-\underline{\Delta})$. The upper bound of Eq. (16) is therefore also valid in this case. For $m=1$, we have $P^{\mathrm{SWN}}[E \mid m=1]=0$. Therefore, with the summation convention adopted above, we may write, for all values of m,

$$P^{\mathrm{SWN}}[E \mid m] \leqslant \sum_{K=0}^{m-2}\binom{L}{K}e^{-\underline{\Delta}\frac{(L-K)}{L}}, \tag{17}$$

so that the total error probability of the SWN receiver is bounded by

$$P_E^{\mathrm{SWN}}[\{\boldsymbol{\alpha}_m\}] \leqslant \sum_{m=1}^{M}\pi_m\sum_{K=0}^{m-2}\binom{L}{K}e^{-\underline{\Delta}\frac{(L-K)}{L}}. \tag{18}$$

A lower bound on the EPE $\xi^{\mathrm{SWN}}[\{\boldsymbol{\alpha}_m\}]$ of the SWN receiver can be obtained by inserting the right-hand side of Eq. (18) into the definition (4) of the EPE. It is readily verified that the EPE depends only on the term decaying the slowest with respect to $\underline{\Delta}$ and we have

$$\begin{aligned}\xi^{\mathrm{SWN}}[\{\boldsymbol{\alpha}_m\}] &\geqslant \frac{\underline{\Delta}}{N}\left(1-\frac{M-2}{L}\right) \\ &= \xi^{\mathrm{Hel}}[\{\boldsymbol{\alpha}_m\}]\left(1-\frac{M-2}{L}\right).\end{aligned} \tag{19}$$

Because we must have $\xi^{\mathrm{SWN}}[\{\boldsymbol{\alpha}_m\}] \leqslant \xi^{\mathrm{Hel}}[\{\boldsymbol{\alpha}_m\}]$ by definition of the Helstrom receiver, we conclude that the EPE of the SWN receiver is at most a factor of $1-(M-2)/L$ away from the Helstrom receiver. If $L<(M-2)$, there are not enough clicks to ever declare the Mth hypothesis (and perhaps other hypotheses as well) and, therefore, $\xi^{\mathrm{SWN}}[\{\boldsymbol{\alpha}_m\}]=0$. On the other hand, in the limit of $L\to\infty$, the two exponents must be identical, establishing the optimality of the SWN receiver exponent in this limit. For a given M, L need not be very large for the EPE to be close to optimal, as seen in the examples in the next section.

C. Performance of the sequential waveform nulling receiver on imaging and communication tasks

We consider the error probability performance of the SWN receiver on three signal sets below. In all cases, we assume that the hypotheses are equally likely, i.e., $\pi_m=1/M$ for all $m\in\{1,\ldots,M\}$.

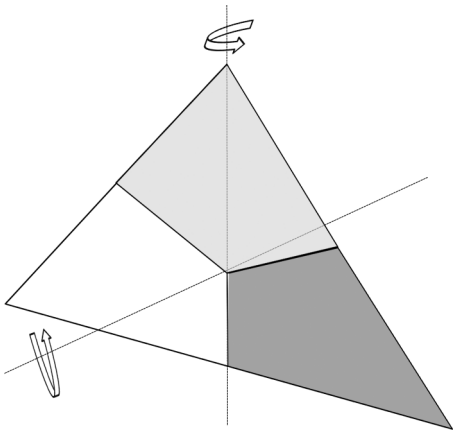

FIG. 2. Hypotheses in an image discrimination problem.

1. Detecting image orientation

Our first example is an image discrimination task with the hypotheses supported on multiple transverse spatial modes. In Fig. 2, the triangular transparency object shown consists of three regions of uniform but unequal phase and amplitude transmissivity.[3] One of the three-fold rotations about the horizontal axis (which is the propagation axis) combined with one of the two-fold rotations about the vertical axis generates six possible orientations of the object. When illuminated by a pulse of transversely uniform coherent-state light propagating on axis, the transparency generates one of six field patterns that constitute the hypotheses to be discriminated. In effect, the output of the receiver is the estimated orientation of the object.

In order to specify the coherent-state set to be discriminated, we fix (arbitrarily) the complex numbers

$$f_1 = \sqrt{\frac{1}{6}}e^{i\pi/3}, \tag{20}$$

$$f_2 = \sqrt{\frac{1}{3}}e^{-i\pi/2}, \tag{21}$$

$$f_3 = \sqrt{\frac{1}{2}} \tag{22}$$

that specify the relative amplitudes of the nonoverlapping spatial modes supported on each of the three regions of the triangle of Fig. 2. The coherent-state ensemble to be discriminated then consists of all permutations among the three spatial modes of the coherent states $|f_1\sqrt{N}\rangle$,$|f_2\sqrt{N}\rangle$, and $|f_3\sqrt{N}\rangle$:

$$\begin{aligned} |\boldsymbol{\alpha}_1\rangle &= |f_1\sqrt{N}\rangle|f_2\sqrt{N}\rangle|f_3\sqrt{N}\rangle, \\ |\boldsymbol{\alpha}_2\rangle &= |f_1\sqrt{N}\rangle|f_3\sqrt{N}\rangle|f_2\sqrt{N}\rangle, \\ &\vdots \\ |\boldsymbol{\alpha}_6\rangle &= |f_3\sqrt{N}\rangle|f_2\sqrt{N}\rangle|f_1\sqrt{N}\rangle, \end{aligned} \tag{23}$$

for average energy N.

[3]The target may alternatively be reflective without affecting the analysis.

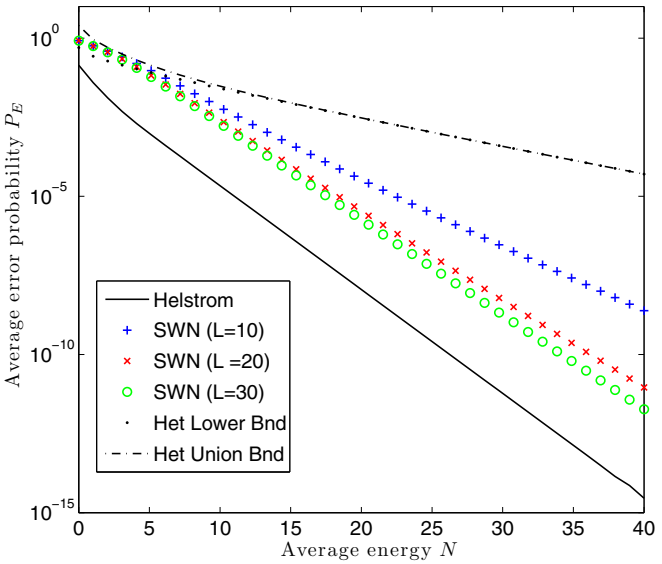

FIG. 3. (Color online) Error probability of various receivers for discriminating a 6-ary coherent-state image set.

The above ensemble is a *geometrically uniform* state set [15] with a non-Abelian generating group (the permutation group S_3) and the optimal measurement is the so-called least-squares measurement (LSM) [18]. In this case (and in the following cases), the LSM is a projective (von Neumann) measurement with orthogonal measurement vectors $\{|\mu_m\rangle\}_{m=1}^M$, and the conditional probability of correct decision given hypothesis m is [18]

$$P[m \mid m] = |\langle\mu_m|\boldsymbol{\alpha}_m\rangle|^2 = (\sqrt{G})_{mm}, \tag{24}$$

where $\sqrt{G}$ is the positive square root of the Gram matrix G of the states defined as

$$G_{mn} = \langle\boldsymbol{\alpha}_m|\boldsymbol{\alpha}_n\rangle. \tag{25}$$

The heterodyne error probability is not available in closed form and so we use the union bound as an upper bound and the bound Eq. (3.7.3) of Ref. [57] as a lower bound. These two bounds have the same exponent and are very close for $N \gtrsim 8$ photons. The exact SWN error probability is calculated from Eq. (13). The performance of these receivers is compared in Fig. 3. We see that the SWN receiver with $L = 10$ slices already beats the heterodyne receiver at $N \gtrsim 6$ photons and that increasing L improves the performance. The $(L = 30)$-SWN receiver has an error probability exponent almost equal to the Helstrom exponent, as evinced by the corresponding curves being nearly parallel.

2. Quadrature phase-shift keying (QPSK)

Consider the 4-ary single-mode signal set (see Fig. 4) with hypotheses corresponding to the coherent states (for average energy N)

$$|\alpha_m\rangle = |i^{(m-1)}\sqrt{N}\rangle; \quad m = 1,\ldots,4. \tag{26}$$

QPSK is a common digital communication format that is becoming popular in optical communication in recent years because it has twice the symbol rate of on-off keying or binary

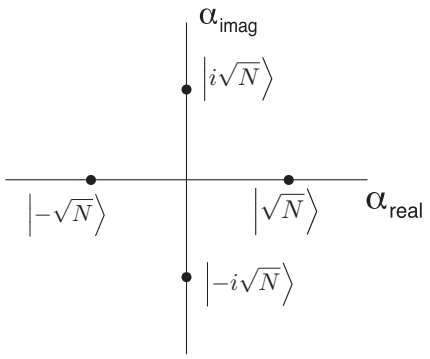

FIG. 4. Quadrature phase-shift keying (QPSK) constellation in phase space.

phase-shift keying [40,58]. In Ref. [33], Bondurant proposed two QPSK receivers, one of which (his "Type-I" receiver) may be regarded as an $L = \infty$ version of our SWN receiver. To see this, note that in Ref. [33], the coherent-states (26) are defined on a flat-top temporal pulse, and the Type-I receiver operates by displacing the input pulse by the negative of the currently nulled hypothesis followed by direct detection on a single-photon detector. When a click is observed, the nulling hypothesis is instantaneously changed to the next in sequence. This receiver is clearly the limiting version of one in which the input pulse is sliced into a very large number of temporal slices of equal width, with the nulled hypotheses being incremented if a click is seen anywhere within a slice duration. Since the pulses are temporally flat, this latter receiver has the same performance (albeit with less decoding delay) to one that slices the input into a very large number of equal-amplitude slices, i.e., the SWN receiver with $L \to \infty$. More recent proposals and experimental implementations of coherent-state QPSK receivers that beat the standard quantum limit may be found in Refs. [34–37].

The plots in Fig. 5 were obtained as follows: The state set (26) is a geometrically uniform state set (in particular,

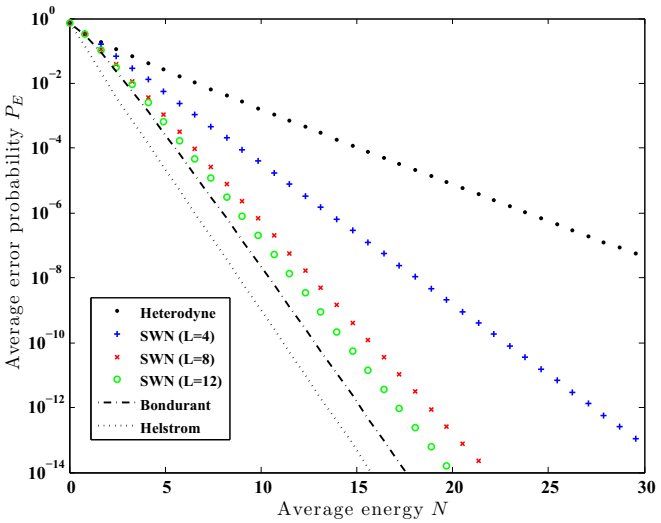

FIG. 5. (Color online) Error probability of various receivers for coherent-state quadrature phase-shift keying (4-PSK).

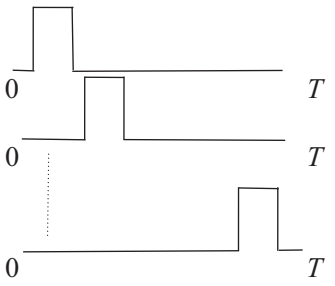

FIG. 6. Temporal waveforms corresponding to pulse position modulation (PPM).

it is a *symmetric set* [14,59]) and, as in the previous case, the Helstrom measurement coincides with the least-squares measurement, and the conditional probability of a correct decision given hypothesis m is given by [15]

$$P[m \mid m] = (\sqrt{G})_{mm}, \tag{27}$$

in terms of the Gram matrix

$$G_{mn} = \langle \alpha_m | \alpha_n \rangle. \tag{28}$$

The error probability of the Type-I Bondurant receiver is taken from Ref. [33]. The error probability of the heterodyne receiver for QPSK is also known in closed form [57]. The SWN error probability for each value of L is obtained from Eq. (13). The superiority of the SWN receiver to the heterodyne receiver is evident from the plots in Fig. 5. Note that increasing L makes the SWN performance approach that of the Type-I Bondurant receiver, as argued to be the case above.

3. *Pulse position modulation*

Consider a single transverse spatial mode and the nonoverlapping temporal modes in the signaling interval $[0,T]$ illustrated in Fig. 6. This signaling set corresponds to pulse position modulation (PPM), another popular modulation format for optical communication [40]. We consider the case of six temporal modes corresponding to the coherent-state ensemble

$$|\boldsymbol{\alpha}_m\rangle = \bigotimes_{k=1}^{6} |\delta_{m,k}\sqrt{N}\rangle, \tag{29}$$

where k indexes the nonoverlapping temporal modes.

The performance of the following receivers on the 6-PPM ensemble is shown in Fig. 7. The Helstrom receiver for M-ary PPM has the error probability [31]

$$P_E^{\text{Hel}} = \frac{M-1}{M^2}\left[\sqrt{1+(M-1)e^{-N}} - \sqrt{1-e^{-N}}\right], \tag{30}$$

the so-called conditional pulse nulling (CPN) receiver has the closed form error probability [31]

$$P_E^{\text{CPN}} = \frac{1}{M}[(1-e^{-N})^M + Me^{-N} - 1], \tag{31}$$

and direct detection has the error probability

$$P_E^{\text{Dir}} = \left(\frac{M-1}{M}\right)e^{-N}. \tag{32}$$

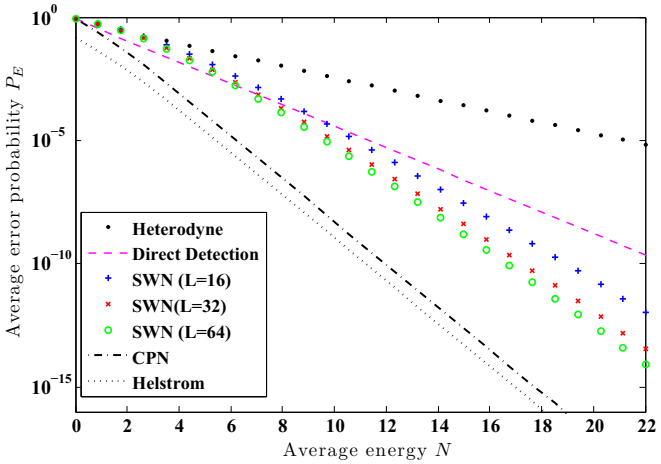

FIG. 7. (Color online) Error probability of various receivers for coherent-state 6-ary pulse position modulation (PPM).

The heterodyne error probability corresponds to that of orthogonal signals in additive white Gaussian noise and can be evaluated numerically [57]. The SWN error probabilities are again calculated via Eq. (13). Note that the CPN receiver's error probability is very close to optimal, while the EPE of the SWN receiver has not yet approached optimal in the photon range shown even for $L = 64$ slices. This near-optimal performance of the CPN receiver stems from its being optimized to the specific structure of the PPM waveforms. We note that the CPN and related receivers have recently been implemented experimentally [32].

V. SEQUENTIAL TESTING RECEIVER

A. Operation

The philosophy of the SWN receiver can be applied to the multicopy discrimination scenario of the M-ary quantum Chernoff bound [50]. Abstractly, the nulling process in the SWN receiver implements a unitary that maps the state $|\boldsymbol{\alpha}_\mu\rangle$ corresponding to the nulled hypothesis to the multimode vacuum state $|\mathbf{0}\rangle$. Detection using a single-photon detector corresponds to a two-outcome POVM $\{|\mathbf{0}\rangle\langle\mathbf{0}|, \mathbb{I} - |\mathbf{0}\rangle\langle\mathbf{0}|\}$. Together, these two steps yield the same statistics as a measurement of the POVM $\{|\boldsymbol{\alpha}_\mu\rangle\langle\boldsymbol{\alpha}_\mu|, \mathbb{I} - |\boldsymbol{\alpha}_\mu\rangle\langle\boldsymbol{\alpha}_\mu|\}$. Now consider a pure-state ensemble $\mathcal{F} = \{|\psi_1\rangle, \ldots, |\psi_M\rangle\}$ of states on an arbitrary Hilbert space $\mathcal{H}$ with prior probabilities $\{\pi_m\}_{m=1}^M$. For each $|\psi_m\rangle$, analogous to the two-element POVM above, define a binary projective POVM on $\mathcal{H}$ via $\Pi_m = |\psi_m\rangle\langle\psi_m|$ and $\Pi_m^\perp = \mathbb{I} - \Pi_m$. The unknown input state $|\psi_m\rangle$ enters the receiver in the n-copy form $\otimes_{l=1}^n |\psi_m\rangle_l$, where we let $1 \leqslant l \leqslant n$ denote the copy index. Analogous to the SWN receiver, we now consider a sequential testing (ST) receiver that operates as follows:

(1) Initialize the *copy index* l to $l = 1$.
(2) Initialize the *current hypothesis* μ to $\mu = 1$.
(3) While $l \leqslant n$,
  (a) Measure $\{\Pi_\mu, \Pi_\mu^\perp\}$ on $|\psi_m\rangle_l$.
  (b) If the $\Pi_\mu^\perp$ outcome is obtained, set $\mu := \mu + 1$.
  (c) $l := l + 1$.
(4) Set the estimated hypothesis $\hat{m} := \mu$.

B. Error probability analysis

In this section, we derive the error probability of the ST receiver, and via an upper bound on this probability, we establish that it attains the M-ary quantum Chernoff exponent in the asymptotic limit.

Analogous to the quantum Chernoff exponent defined in Eq. (5), we may define the multicopy error exponent $\xi^{\mathrm{ST}}[\mathcal{F}]$ of the ST receiver as

$$\xi^{\mathrm{ST}}[\mathcal{F}] := -\lim_{n\to\infty} \frac{1}{n} \ln P_E^{\mathrm{ST}}[\mathcal{F}^{\otimes n}], \tag{33}$$

where $P_E^{\mathrm{ST}}[\mathcal{F}^{\otimes n}]$ is the average error probability of the ST receiver for discriminating the ensemble $\mathcal{F}^{\otimes n}$.

The performance analysis of the ST receiver follows largely the same lines as that of the SWN receiver. Because making the $\{\Pi_m, \Pi_m^\perp\}$ measurement on $|\psi_m\rangle$ can never lead to a "$\perp$" outcome, we have

$$P^{\mathrm{ST}}[E \mid m] = \sum_{K=0}^{m-2} \Pr[K \text{ " } \perp \text{ " outcomes} \mid m]. \tag{34}$$

As before, for each $K > 0$, we define a length-K vector $\mathbf{l} = (l_1, \ldots, l_K)$ whose kth component l_k is the copy number in the detection of which the kth "$\perp$" outcome occurred. We may then write

$$\begin{aligned}
&\Pr[K \text{ " } \perp \text{ " outcomes} \mid m] \\
&\quad = \sum_{\text{allowed}\mathbf{l}} |\langle\psi_1|\psi_m\rangle|^{2(l_1-1)}[1 - |\langle\psi_1|\psi_m\rangle|^2] \\
&\qquad \times |\langle\psi_2|\psi_m\rangle|^{2(l_2-l_1-1)}[1 - |\langle\psi_2|\psi_m\rangle|^2] \times \cdots \\
&\qquad \times [1 - |\langle\psi_K|\psi_m\rangle|^2]|\langle\psi_{K+1}|\psi_m\rangle|^{2(n-l_K)} \qquad (35) \\
&\quad \leqslant \sum_{\text{allowed}\mathbf{l}} F_{\max}^{(l_1-1)} F_{\max}^{(l_2-l_1-1)} \times \cdots \times F_{\max}^{(n-l_K)} \qquad (36) \\
&\quad = \sum_{\text{allowed}\mathbf{l}} F_{\max}^{(n-K)} = \binom{n}{K} F_{\max}^{(n-K)}, \qquad (37)
\end{aligned}$$

where

$$F_{\max} = \max_{m,m':m\neq m'} |\langle\psi_m|\psi_{m'}\rangle|^2, \tag{38}$$

and Eq. (37) happens to also be valid for $K = 0$. The average error probability of the ST receiver can then be bounded as

$$\begin{aligned}
P_E^{\mathrm{ST}}[\{|\psi_m\rangle^{\otimes n}\}] &= \sum_{m=1}^M \pi_m P^{\mathrm{ST}}[E \mid m] \\
&\leqslant \sum_{m=1}^M \pi_m \sum_{K=0}^{m-2} \binom{n}{K} F_{\max}^{(n-K)}.
\end{aligned} \tag{39}$$

A lower bound on the Chernoff error exponent ξ^{ST} of the ST receiver can be obtained by inserting the right-hand side of Eq. (39) into Eq. (33). Factoring out the lowest power of $F_{\max}$

on the right-hand side, namely $F_{\max}^{n-M+2}$, we have

$$-\frac{1}{n}\ln P_E^{\mathrm{ST}}[\{|\psi_m\rangle^{\otimes n}\}] \geqslant -\frac{n-M+2}{n}\ln F_{\max} - \frac{1}{n}\ln\left[\sum_{m=1}^{M}\pi_m\sum_{K=0}^{m-2}\binom{n}{K}F_{\max}^{(M-K-2)}\right]. \tag{40}$$

Since $\pi_m \leqslant 1$, $\binom{n}{K} \leqslant n^K$, and $F_{\max} < 1$, we may bound the argument of the logarithm in the second term as

$$\sum_{m=1}^{M}\pi_m\sum_{K=0}^{m-2}\binom{n}{K}F_{\max}^{(M-K-2)} \leqslant M^2 n^{M-2}. \tag{41}$$

Substituting this back into Eq. (40) gives

$$-\frac{1}{n}\ln P_E^{\mathrm{ST}}[\{|\psi_m\rangle^{\otimes n}\}] \geqslant -\frac{n-M+2}{n}\ln F_{\max} - \frac{\ln M^2}{n} - (M-2)\frac{\ln n}{n}. \tag{42}$$

Taking the limit of $n \to \infty$, we have

$$\xi^{\mathrm{ST}}[\{|\psi_m\rangle\}] \geqslant -\ln F_{\max} = \xi_{\mathrm{QC}}[\{|\psi_m\rangle\}]. \tag{43}$$

Since $\xi_{\mathrm{QC}}[\{|\psi_m\rangle\}]$ is the maximum exponent allowed of any receiver, we must have

$$\xi^{\mathrm{ST}}[\{|\psi_m\rangle\}] = \xi_{\mathrm{QC}}[\{|\psi_m\rangle\}], \tag{44}$$

so that the ST receiver achieves the quantum Chernoff exponent in the asymptotic limit of many copies.

VI. DISCUSSION AND OUTLOOK

We have used an amplitude-splitting argument to derive the quantum-optimal EPE for discriminating M coherent states—such an argument connects the two notions of EPE pertaining to signal energy and number of copies that were defined in Sec. II. A similar splitting argument was used in Ref. [60] to rederive the Dolinar receiver [21] for discriminating two coherent states from multicopy binary discrimination [43]. Implementing the SWN receiver requires beam splitters, the ability to coherently engineer spatiotemporal coherent-state waveforms, and single-photon detection—all these operations are currently available in the laboratory. Remarkably, this limited toolbox achieves the optimal error probability exponent allowed by quantum mechanics on arbitrary spatiotemporal coherent states. The SWN receiver may be applied to unamplified communication links, such as space and satellite links, and for metrology and imaging using laser light. Its superior performance to conventional receivers translates to lower energy requirements for tasks like imaging biological cells, where noninvasiveness is important. As with all coherent receivers, a major challenge in implementing the SWN receiver is to maintain phase and amplitude coherence between the received signal and LO waveforms. In practice, this may be achieved using phase and amplitude recovery from a strong pilot pulse in a different mode than the signals. Since the SWN receiver relies on exact cancellation when the LO and signal states are identical, quantifying the effect of imperfections in the nulling process arising from lack of perfect control of the LO waveforms is of interest. The absolute performance of the receiver may be further improved by adapting the sequence of nulling hypotheses based on measurement data [33–35,42–47]. In general, however, we may expect the SWN and similar cancellation-based receivers to be quite sensitive to noise either from the above sources or due to background photons, since these can cause the nulled hypotheses to be spuriously incremented leading to error. Therefore, no general optimality of the SWN receiver is likely to hold in noisy cases. Analyses of these aspects and extensions of the SWN receiver is left for future work.

The ST receiver provides an alternative proof to that in Ref. [50] of the achievability of the M-ary quantum Chernoff exponent for pure states (the LOCC achievability of the $M = 2$ case was studied in Ref. [43]). It is remarkable that it does so using only copy-by-copy binary measurements and feedforward, unlike the joint measurement used in Ref. [50]. The measurements on each copy can be destructive and are, for example, readily made on polarization-encoded photonic qubits [44]. It should be interesting to explore the capabilities of LOCC measurements for discrimination of M-ary mixed-state ensembles in the asymptotic limit.

ACKNOWLEDGMENTS

We thank A. Chia, M. Nussbaum, M. Tsang, H. M. Wiseman, and B. J. Yen for useful discussions. R.N. is supported by the Singapore National Research Foundation under Grant No. NRF-NRFF2011-07, S.G. by the DARPA Information in a Photon (InPho) program under contract number HR0011-10-C-0162, and S.-H. T. by the Data Storage Institute, Singapore and by the Singapore National Research Foundation under NRF Award No. NRF-NRFF2013-01.

[1] C. W. Helstrom, *Quantum Detection and Estimation Theory* (Academic Press, New York, 1976).
[2] A. Chefles, Contemp. Phys. **41**, 401 (2000).
[3] S. M. Barnett and S. Croke, Adv. Opt. Photonics **1**, 238 (2009).
[4] H. M. Wiseman and G. J. Milburn, *Quantum Measurement and Control* (Cambridge University Press, Cambridge, UK, 2010).
[5] S.-H. Tan, B. I. Erkmen, V. Giovannetti, S. Guha, S. Lloyd, L. Maccone, S. Pirandola, and J. H. Shapiro, Phys. Rev. Lett. **101**, 253601 (2008).
[6] S. Pirandola, Phys. Rev. Lett. **106**, 090504 (2011).
[7] M. Tsang, Phys. Rev. Lett. **108**, 170502 (2012).
[8] M. Tsang and R. Nair, Phys. Rev. A **86**, 042115 (2012).

[9] N. Gisin *et al.*, Rev. Mod. Phys. **74**, 145 (2002).
[10] H. P. Yuen, IEEE J. Sel. Top. Quantum Electron. **15**, 1630 (2009).
[11] W. Matthews, S. Wehner, and A. Winter, Commun. Math. Phys. **291**, 813 (2009).
[12] H. P. Yuen, R. S. Kennedy, and M. Lax, IEEE Trans. Inf. Theory **21**, 125 (1975).
[13] S. M. Barnett and S. Croke, J. Phys. A **42**, 062001 (2009).
[14] M. Ban, K. Kurokawa, R. Momose, and O. Hirota, Int. J. Theor. Phys. **36**, 1269 (1997).
[15] Y. C. Eldar and G. D. Forney, Jr., IEEE Trans. Inf. Theory **47**, 858 (2001).
[16] S. M. Barnett, Phys. Rev. A **64**, 030303 (2001).
[17] C.-L. Chou and L. Y. Hsu, Phys. Rev. A **68**, 042305 (2003).
[18] Y. C. Eldar, A. Megretski, and G. C. Verghese, IEEE Trans. Inf. Theory **50**, 1198 (2004).
[19] R. Blume-Kohout, S. Croke, and M. Zwolak, Tech. Rep. LA-UR 12-00400 (Los Alamos Reports, 2012); arXiv:1201.6625v1.
[20] R. S. Kennedy, *A Near-Optimum Receiver for the Binary Coherent State Channel*, Tech. Rep. 108 (MIT RLE Quarterly Progress Report, 1973).
[21] S. J. Dolinar, *An Optimum Receiver for the Binary Coherent State Channel*, Tech. Rep. 111 (MIT RLE Quarterly Progress Report, 1973).
[22] R. L. Cook, P. J. Martin, and J. M. Geremia, Nature (London) **446**, 774 (2007).
[23] M. Sasaki and O. Hirota, Phys. Rev. A **54**, 2728 (1996).
[24] M. Takeoka, Opt. Spectrosc. **103**, 98 (2007).
[25] M. Takeoka, M. Sasaki, and N. Lütkenhaus, Phys. Rev. Lett. **97**, 040502 (2006).
[26] M. Takeoka, M. Sasaki, P. van Loock, and N. Lütkenhaus, Phys. Rev. A **71**, 022318 (2005).
[27] M. Takeoka and M. Sasaki, Phys. Rev. A **78**, 022320 (2008).
[28] C. Wittmann, M. Takeoka, K. N. Cassemiro, M. Sasaki, G. Leuchs, and U. L. Andersen, Phys. Rev. Lett. **101**, 210501 (2008).
[29] K. Tsujino *et al.*, Opt. Express **18**, 8107 (2010).
[30] K. Tsujino, D. Fukuda, G. Fujii, S. Inoue, M. Fujiwara, M. Takeoka, and M. Sasaki, Phys. Rev. Lett. **106**, 250503 (2011).
[31] S. J. Dolinar, *Tech. Rep. 42–72, Telecom. and Data Acquisition Progress Report* (NASA, Pasadena, 1982).
[32] J. Chen *et al.*, Nat. Photonics. **6**, 374 (2012).
[33] R. S. Bondurant, Opt. Lett. **18**, 1896 (1993).
[34] F. E. Becerra, J. Fan, G. Baumgartner, S. V. Polyakov, J. Goldhar, J. T. Kosloski, and A. Migdall, Phys. Rev. A **84**, 062324 (2011).
[35] F. E. Becerra *et al.*, Nat. Photonics **7**, 147 (2013).
[36] C. R. Müller *et al.*, New J. Phys. **14**, 083009 (2012).
[37] S. Izumi, M. Takeoka, M. Fujiwara, N. D. Pozza, A. Assalini, K. Ema, and M. Sasaki, Phys. Rev. A **86**, 042328 (2012).
[38] M. P. da Silva, S. Guha, and Z. Dutton, Phys. Rev. A **87**, 052320 (2013).
[39] R. J. Glauber, Phys. Rev. **131**, 2766 (1963).
[40] R. M. Gagliardi and S. Karp, *Optical Communications*, 2nd ed. (John Wiley & Sons, New York, 2000).
[41] K. J. Gåsvik, *Optical Metrology*, 3rd ed. (John Wiley & Sons, Chichester, England, 2002).
[42] D. Brody and B. Meister, Phys. Rev. Lett. **76**, 1 (1996).
[43] A. Acín, E. Bagan, M. Baig, L. Masanes, and R. Munoz-Tapia, Phys. Rev. A **71**, 032338 (2005).
[44] B. L. Higgins, B. M. Booth, A. C. Doherty, S. D. Bartlett, H. M. Wiseman, and G. J. Pryde, Phys. Rev. Lett. **103**, 220503 (2009).
[45] M. Hayashi, IEEE Trans. Inf. Theory **55**, 3807 (2009).
[46] J. Calsamiglia, J. I. de Vicente, R. Muñoz-Tapia, and E. Bagan, Phys. Rev. Lett. **105**, 080504 (2010).
[47] B. L. Higgins, A. C. Doherty, S. D. Bartlett, G. J. Pryde, and H. M. Wiseman, Phys. Rev. A **83**, 052314 (2011).
[48] M. Nussbaum and A. Szkoła, Ann. Stat. **37**, 1040 (2009).
[49] K. M. R. Audenaert, J. Calsamiglia, R. Muñoz-Tapia, E. Bagan, Ll. Masanes, A. Acin, and F. Verstraete, Phys. Rev. Lett. **98**, 160501 (2007).
[50] M. Nussbaum and A. Szkoła, in *Proceedings of TQC 2010, Leeds, UK*, Lecture Notes Computer Science (Springer Verlag, 2011), Vol. 6519, p. 1.
[51] M. Nussbaum and A. Szkoła, Ann. Stat. **39**, 3211 (2011).
[52] M. Nussbaum, in *Proceedings of 1st International Workshop on Entangled Coherent States 2012, Tokyo, Japan*, edited by T. S. Usuda and K. Kato (2013), p. 77, arXiv:1308.6563.
[53] H. Chernoff, Ann. Math. Stat. **23**, 493 (1952).
[54] J. H. Shapiro, IEEE J. Sel. Top. Quantum Electron. **15**, 1547 (2009).
[55] N. P. Salikhov, Theory Probab. Its Appl. (Engl. Transl.) **43**, 239 (1999).
[56] H. L. Van Trees, *Detection, Estimation, and Modulation Theory: Part I*, 1st ed. (Wiley-Interscience, New York, 2001).
[57] A. J. Viterbi and J. K. Omura, *Principles of Digital Communication and Coding* (Dover Books on Electrical Engineering, Dover Publications, Mineola, NY, 2009).
[58] G. P. Agrawal, *Fiber-Optic Communication Systems*, 4th ed., Wiley Series in Microwave and Optical Engineering (Wiley, Hoboken, NJ, 2010).
[59] K. Kato, M. Osaki, M. Sasaki, and O. Hirota, IEEE Trans. Comm. **47**, 248 (1999).
[60] A. Assalini, N. Dalla Pozza, and G. Pierobon, Phys. Rev. A **84**, 022342 (2011).